MDPI

Article

Morphodynamic Evolution of Post-Nourishment Beach Scarps in Low-Energy and Micro-Tidal Environment

Gen Liu [1,2,3], Hongshuai Qi [1,2,3], Feng Cai [1,2,3,*], Jun Zhu [1,2,3], Gang Lei [1,2,3], Jianhui Liu [1,2,3], Shaohua Zhao [1] and Chao Cao [1,2,3]

[1] Third Institute of Oceanography, Ministry of Natural Resources, Xiamen 361005, China; liugen@tio.org.cn (G.L.); qihongshuai@tio.org.cn (H.Q.); junzhu@tio.org.cn (J.Z.); leigang@tio.org.cn (G.L.); liujianhui@tio.org.cn (J.L.); zhaoshaohua@tio.org.cn (S.Z.); caochao@tio.org.cn (C.C.)
[2] Fujian Provincial Key Laboratory of Marine Ecological Conservation and Restoration, Xiamen 361005, China
[3] Southern Marine Science and Engineering Guangdong Laboratory (Zhuhai), Zhuhai 591000, China
* Correspondence: caifeng@tio.org.cn

Abstract: Beach scarps are commonly associated with nourishment. Large and persistent beach scarps not only affect the performance of beach nourishment, but also are safety hazards to tourists. In this study, the morphological evolution of beach scarps was examined at a nourished beach in a low-energy and micro-tidal environment. Topographic surveys of nine beach profiles were carried out every 3–6 months after nourishment, lasting for nearly 4.5 years, combined with observed and simulated hydrodynamic data. The results showed that beach scarps were extensively developed after nourishment and migrated landward gradually. The formation of beach scarps was attributed to the higher designed berm, while the migration was possibly initiated by the subsequent higher total water level connected with the irregular tides. However, scarps were completely removed by the first post-nourishment severe storm and had been long absent ever since although two other energetic storms approached. This was different from the result of previous studies, which could be attributed to the much gentler upper beach slope. These results highlighted that the first post-nourishment storm played a key role in the evolution of beach scarps at low-energy and micro-tidal nourished beaches. This study also proposed two methods of determining berm elevation in beach nourishment according to China's experiences, which would be helpful for other countries' beach nourishment projects.

Keywords: morphodynamics; total water level; storm; slope; berm

1. Introduction

Beach scarps are defined as a nearly vertical discontinuity in the foreshore slope. As a distinctive morphological feature of many shorelines [1], they are often associated with coastal erosion [2,3]. A beach scarp was defined as a feature with a slope larger than the critical angle of repose of 32° and a minimum height of 0.25 m [4]. They can be as high as 3 m [5] and extended for thousands of meters along the shoreline [1]. Higher beach scarps cause inconvenience and pose serious safety hazards to beach users [4,6]. Beach scarps have been reported around the world [3], not only along natural shorelines [6–8], but also on nourished beaches shortly after implementation [3,4,9–13].

The morphodynamic of beach scarps mainly involves three aspects, i.e., the formation, migration, and destruction. Various factors are responsible for the formation of beach scarps. Two groups of reasons for scarp formation was proposed by Sherman and Nordstrom [1], one is the changing nearshore processes, including increased wave height, wind, tidal currents, and angle of wave approach, and the other is the alongshore variability induced by coastal structures or natural headlands. For example, an increase in wave height will remove sediment and cause the lower beach to be flattened while the upper beach remains unchanged. Then, a discontinuity emerges between the upper and lower beach.

If the discontinuity continues and expands, a scarp will be formed. Scarp formation can also be attributed to energetic conditions, e.g., storms [3,5]. The migration of scarps was mainly related to the swash impacts, regulated by the runup elevation [5]. The persistency of beach scarps depends on wave overtopping events during high water level and storm wave heights [12,14]. The destruction of beach scarps can be classified into four general mechanisms, hydrodynamically controlled overwash or inundation, drying collapse, burying by aeolian transport, and swash deposition [5].

However, the knowledge of beach scarp evolution and their morphodynamics on nourished beaches are poorly understood. A few researches have focused on the beach scarps of nourished beaches [5,12,14–16]. Beach scarps can be formed due to the inadequate design of the nourished beach profile shape [12,14] or a different grain size of filling sediment to that of the origin [4], or attributed to the steep nearshore beach profile present after the nourishment [3,5]. Beach scarp toe elevation is related to the total wave runup and the destruction of scarps can be explained by the water levels exceeding the scarp top [5]. Authors found that beach scarp still form after storms at nourished beaches [12,16]. Van Bemmelen et al. [5] also found that the formation of beach scarps in nourishment cases was linked to mildly erosive (summer storm) conditions, whereas the destruction was related to extremely erosive (winter storm) conditions. It seemed that storms can induce both the formation and destruction of beach scarps on nourished beaches. The processes that induce the generation, migration, and destruction of beach scarps associated with beach nourishment in low-energy and micro-tidal environments are still not well understood due to fewer studies [5,7,12,17]. Especially, the role of storms in beach scarp behaviors in micro-tidal environments has not been well studied. On micro-tidal coasts, storms commonly induced overwash or inundation, in contrast to that overwash seldom occurs on macro-tidal coasts [18]. The overwash or inundation mechanism may be a key process that controls the evolution of beach scarps.

South China is frequently susceptible to storms. This paper focuses on a nourished beach along a low-energy and micro-tidal coast, located on the western coast of the Pearl River Estuary, China, and aims to examine the evolution of beach scarps over medium-term timescale and to explore the role of storms in beach scarp behaviors. Understanding the morphodynamics of beach scarp provide insight into the mechanism of nourished beach change since scarps commonly form after nourishment. Knowledge of beach scarp behaviors will also help estimate their dimension and persistency, which is beneficial to coastal engineers for better design in beach nourishment.

2. Study Site

Meili bay (ML bay) is a headland bay, located on the western coast of the Pearl River Estuary, China (Figure 1a). Meili bay is characterized by long and wide sandy beaches in the past century. However, the beaches disappeared due to coastal reclamation with increasing urbanization [19]. At the end of 2015, a large beach nourishment project was implemented on the northern segment of ML bay by local government to construct an artificial beach, i.e., Meiliwan beach (ML beach). This beach nourishment project was designed for shore protection of property from storm damage and space for beach recreation. A total of 248,000 m^3 of sand was placed on a 1090-m-long beach to create a 45-m-wide berm. The nourished beach spanned from NE to SW, which was bounded by a drainpipe to the northeast and a small headland to the southwest. During this project, a drainage culvert in the middle of the beach was also extended seaward, interrupting the long beach (Figure 1b,c). The height of the constructed beach berm was 3.0 m above the local mean sea level (msl) and the initial slope of the foreshore was 0.17. Native sediment at ML beach is a medium ($M_\Phi = 1.52$) and well sorted ($\sigma_\Phi = 0.5$) sand, while the filled sediment is a bit finer ($M_\Phi = 1.59$) and less sorted ($\sigma_\Phi = 0.76$) (Figure 2a). Furthermore, the calculated Stability Index (Si) of the filled sediment was approximately 0.50, showing that the filled sediment was appropriate [20]. ML beach presented a low-tide terrace profile, with a steep sandy intertidal zone and a gentle muddy subtidal zone.
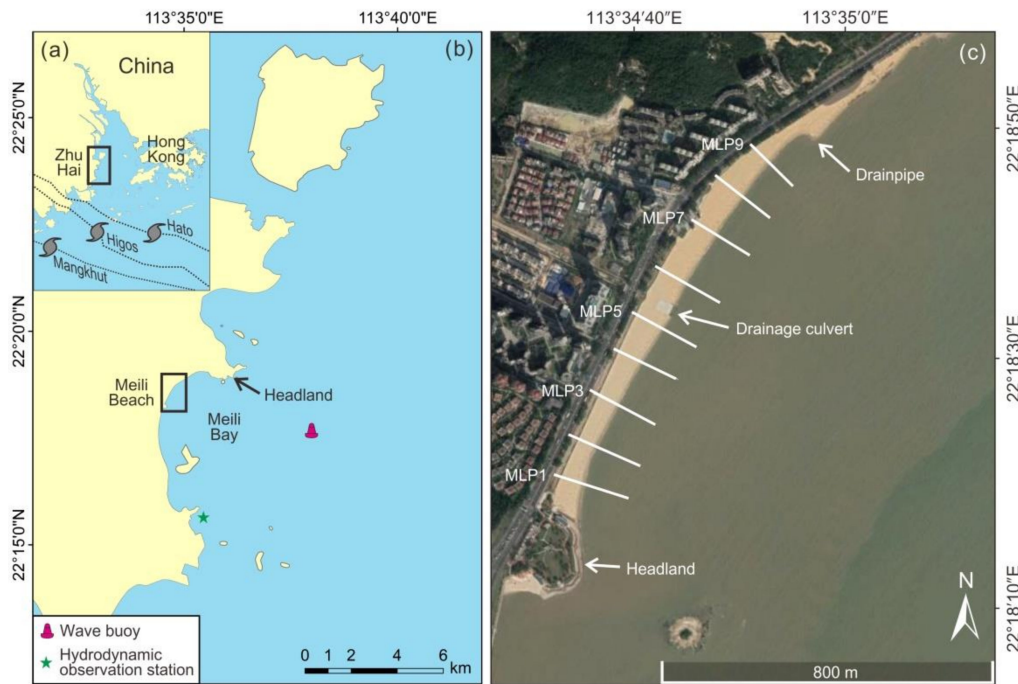
Figure 1. Location map of Meili (ML) beach and associated beach profiles. The dotted lines in (**a**) indicate the tracks of three energetic typhoons affecting this beach since 2016. The locations of the wave buoy and hydrodynamic observation station are showed in (**b**), whereas the white lines in (**c**) indicate the monitored beach profiles. The image in (**c**) is from Google Earth, taken in February 2019.
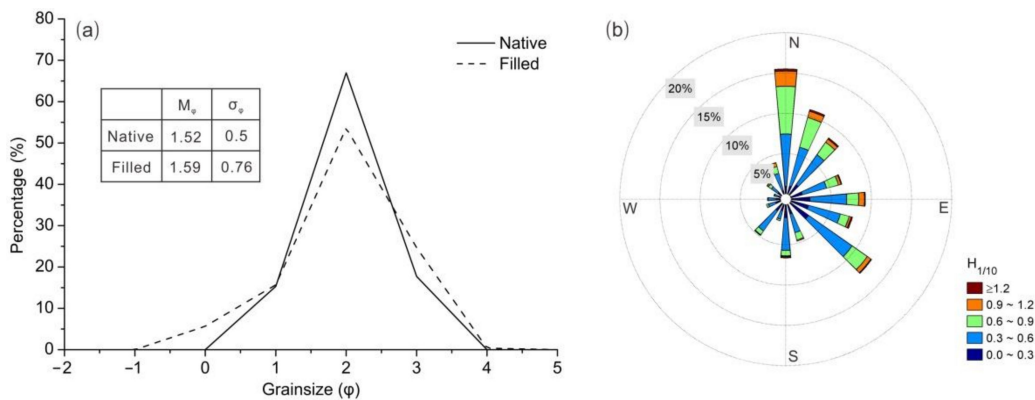

Figure 2. The grainsize distribution for native and borrow sediments (**a**) and rose diagram of annual waves observed from 1 August 2013 to 31 July 2014 near ML beach (**b**).

Tides at ML beach are irregularly semi-diurnal with a mean range of 1.2 m and a spring range of 2.2 m. The active foreshore is normally about 25 m wide during spring tides. The annual offshore waves show that the dominant waves approach from the north and southeast most of the year. The wave climate also exhibits a seasonal variation. The predominant wave directions are from the southeast in spring and summer and north/northeast in autumn and winter [21]. Nearly all of the incident waves are of low-energy, characterized by a wave height ($H_{1/10}$) of less than 1.0 m (Figure 2b). The average value of $H_{1/10}$ throughout the year is 0.38 m, and the associated wave period is 3.6 s [19]. The nearshore wave crest is nearly parallel with the coastline, just resulting in a slight southwestward net longshore transport to the north of the drainage culvert [21].

Since nourishment, three energetic storms had impacted ML beach significantly. Typhoon Hato in 2017 was the first energetic storm affecting ML beach after nourishment, which was considered as one of the strongest tropical cyclones to make landfall in Southern

China since 1947 [22]. Typhoon Hato hit ML Beach at 12:50 UTC+8 on 23 August 2017, with a maximum wind speed of 45 m/s near the cyclone center [23]. Since the time of Hato's landing coincided with the astronomical high water level of spring tide, strong winds and storm surges resulted in a maximum water level of 3.7 m (msl). Another energetic storm, i.e., Typhoon Mangkhut, made landfall in Jiangmen, 70 km away from ML Beach, at 17:00 UTC+8 on 16 September 2018 with a maximum wind speed of 45 m/s near the cyclone center [24]. A maximum water level of 3.3 m (msl) was recorded during Mangkhut, causing an inundation depth of approximately 0.3 m at ML beach. The third storm, Typhoon Higos made its landfall in Zhuhai at 06:00 UTC+8 on 19 August 2020, with a maximum wind speed of 35 m/s near the cyclone center. Higos induced a storm surge of 1.0 m, coinciding with the spring tide.

3. Materials and Methods

3.1. Beach Topography

Nine beach profiles, perpendicular to the shoreline, were set and monitored along ML beach, numbered from MLP1 in the southwest to MLP9 in the northernmost (Figure 1c). These profiles were spaced roughly 130 m alongshore. Beach topography measurement started from March 2016, 2 months after nourishment, and continued for over 4 years until August 2020. A total of 17 repeated surveys were implemented with a time interval of 3–6 months. These measurements were conducted by a Trimble RTK GPS with horizontal and vertical accuracies of less than 2 cm. Beach profile topography was surveyed from the seawall to a fording depth during the low water level of spring tides.

3.2. Beach Scarp Identification

Beach scarps can be detected by examining the slope variation of a cross-shore beach profile [4] or visual inspection of topographic data [3]. In this study, beach scarps are identified following the method of de Alegria-Arzaburu et al. [4]. The top and toe positions of beach scarps are calculated from the minimum and maximum values of the second derivative of the measured beach profiles, respectively [4]. The scarp height is the vertical elevation difference between the top and toe. Furthermore, the upper and middle beach slopes are calculated to explore the relationship between slopes and scarp formation. The upper beach slope (α), is defined as the linear slope between the scarp top (berm crest) and the toe (upper slope break), while the middle beach slope (β) between the scarp toe and the lower slope break (Figure 3).
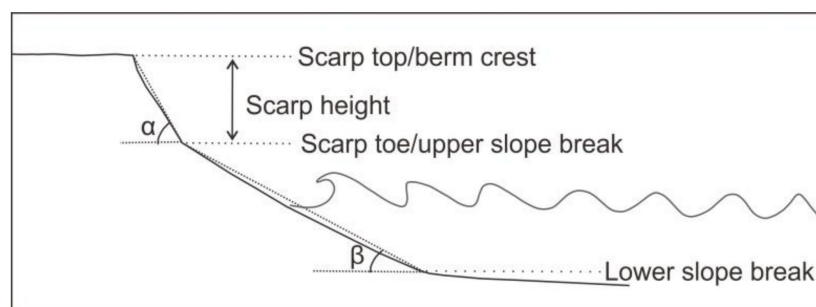

Figure 3. Definition sketch for beach scarps and associated slopes. α and β are the upper and middle beach slope, respectively.

3.3. Hydrodynamic Data

Beach scarp evolution is examined with respect to the time-series total water level on the beach. We failed to acquire the long-term continuous time-series (covering the entire survey period) of nearshore waves and water levels at ML beach. However, a whole year of nearshore waves and water levels in 2017 was obtained by numerical simulation. Nearshore waves at ML beach are transformed by MIKE21 Spectral Waves (Danish Hydraulic Institute, Hørsholm, Denmark) from the WaveWatch III (NOAA/NCEP, Silver Spring, United States)

and verified by the nearby offshore wave station, approximately 8 km south from ML beach (Figure 4). The time-series of astronomical tidal levels is derived by the MIKE21 Tidal Analysis and Prediction Module (Figure 4). Moreover, the nearshore water level (including storm surge) and significant wave height at ML beach during Typhoon Hato (2017) and Mangkhut (2018) are observed at a coastal observation station (indicated in Figure 1b) and these data are obtained (Figure 5).
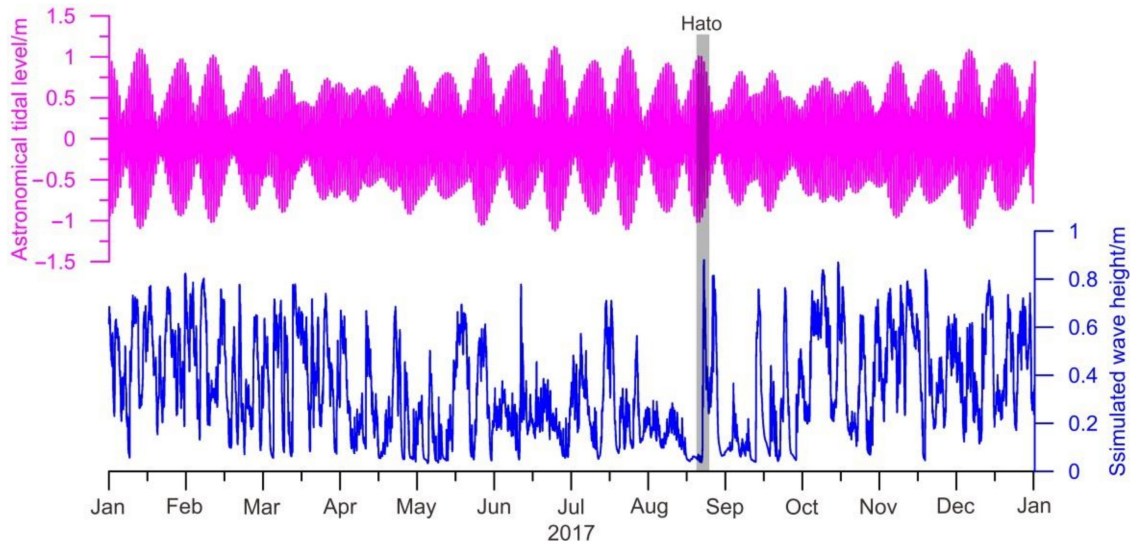

Figure 4. Derived astronomical tidal levels (**upper panel**) and simulated wave heights (**lower panel**) near ML beach during 2017. Grey band highlights the period in which Typhoon Hato approached.
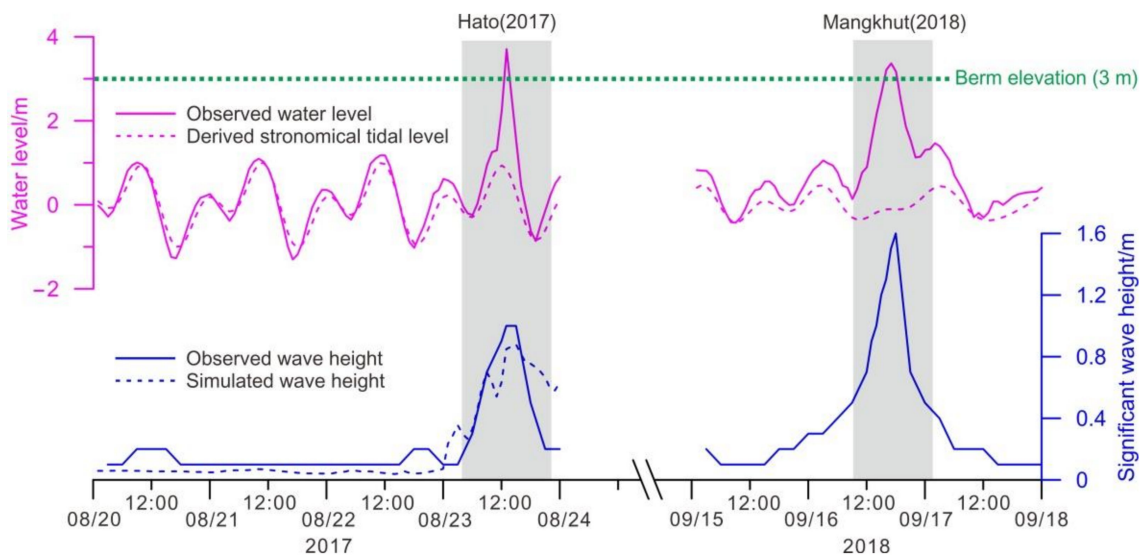

Figure 5. Observed and simulated water levels (**upper panel**) and significant wave heights (**lower panel**) near ML beach during Typhoon Hato (2017) and Mangkhut (2018). Grey bands highlight the period in which storms induced significant hydrodynamic variation.

These wave data, combined with the beach slope, are used to estimate the wave runup using Stockdon et al. [25]:

$$R_{2\%} = 1.1\left\{0.35\beta(H_0L_0)^{1/2} + \frac{\left[H_0L_0(0.563\beta^2 + 0.004)\right]^{1/2}}{2}\right\} \tag{1}$$

where $R_{2\%}$ is the 2% exceedance wave runup in meters, β is the foreshore slope, H_0 is the offshore wave height, and L_0 is the offshore wave length ($L_0 = gT^2/2\pi$). The foreshore slope corresponds to the middle beach slope, as defined in Figure 3, and is determined as the average slope along the nine beach profiles over the study period.

Total water level (η) is then estimated by the combination of the observed water level with the wave runup ($R_{2\%}$) or by the combination of the derived astronomical tidal level, wave setup, and wave runup ($R_{2\%}$).

4. Results

4.1. Beach Profile Changes

Figure 6 illustrated three examples of long-term beach profile morphology change from March 2016 to August 2020. Results showed that beach scarps were generally formed at the seaward edge of the artificial berm after nourishment. Due to the presence of these scarps, a slope break was present at the foreshore beach, dividing the profile into two entirely different portions (Figure 7b). The initial scarps had a larger height, as much as 1.2 m (Figure 7a). A persistent presence and slight landward retreat of these scarps was observed between March 2016 and May 2017 (Figure 7c,d). During this period, the foreshore beach was gradually flattened with the landward retreat of these scarps. However, all the scarps disappeared when Typhoon Hato made its landfall at ML beach in August 2017 (Figure 7e). After Hato, the upper foreshore eroded notably and the beach berm retreated for approximately 20 m, especially in the southern segment (MLP2 and MLP4). Since Hato, no beach scarps had been observed at ML beach in spite of two other energetic storms attacking ML beach (Figure 7f–h).
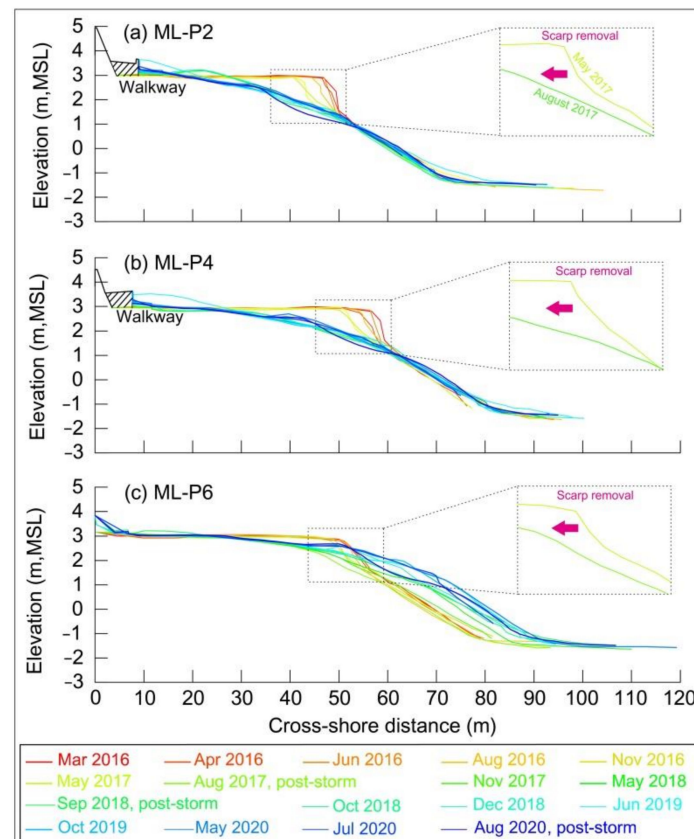

Figure 6. Examples of time-series beach profile morphology changes from March 2016 to August 2020, showing the evolution of scarps. The enlarged inserts highlighted the scarp removal after the first post-nourishment energetic storm (Typhoon Hato) in August 2017.
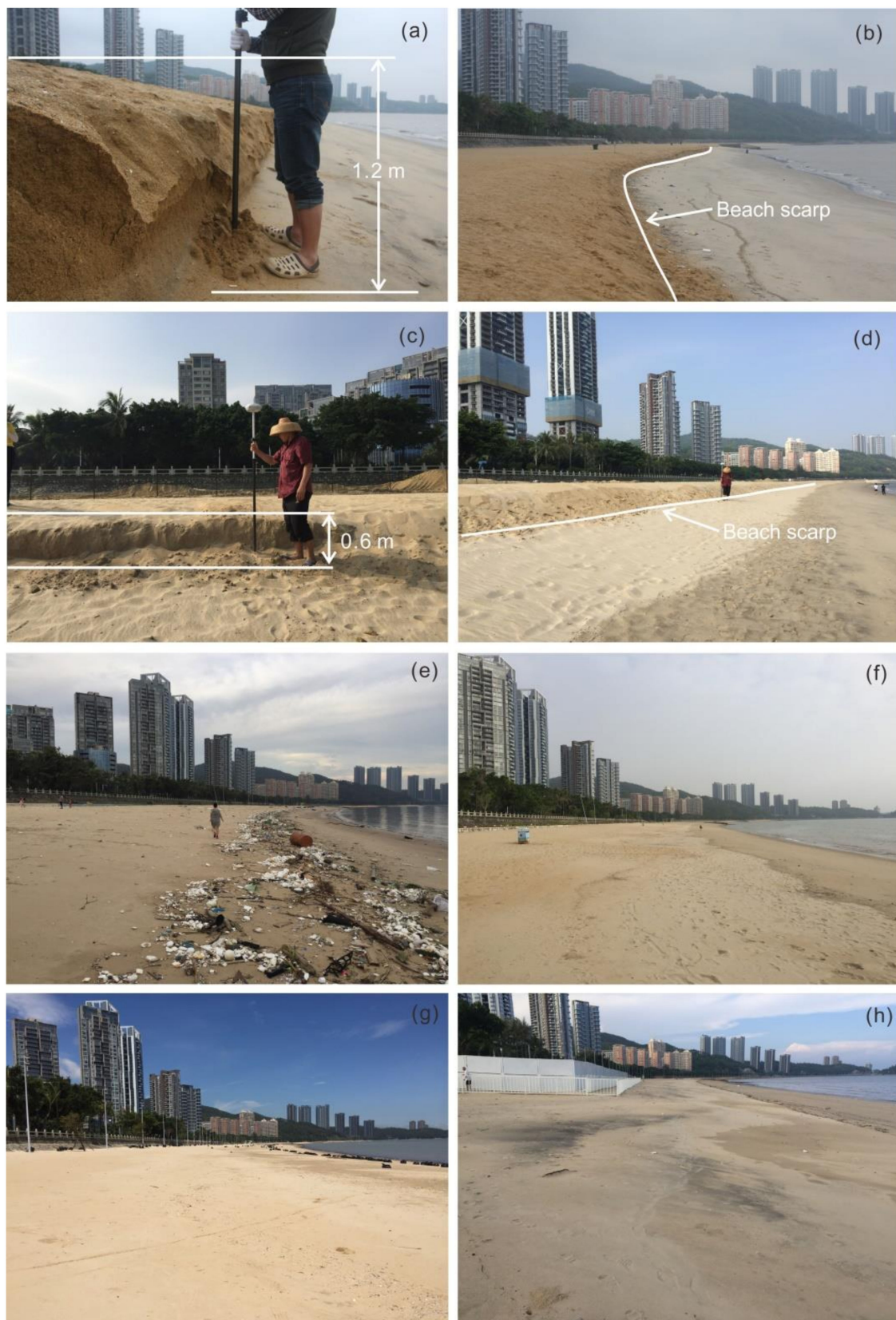
Figure 7. The presence and absence of beach scarp at different periods. March 2016 (**a**,**b**), November 2016 (**c**,**d**), August 2017, post-storm Hato (**e**), November 2017 (**f**), September 2018, post-storm Mangkhut (**g**), and August 2020, post-storm Higos (**h**).

4.2. Beach Scarp Changes

The temporal variability revealed the evolution of beach scarps from formation, to migration, and to destruction alongshore (Figure 8). Results showed that beach scarps were present at all of the nine profiles for the first survey in March 2016, two months after nourishment. The initial scarps had a relatively larger dimension with height ranging from 1.1 m to 1.3 m, revealing an alongshore variability of these scarps. Then between March 2016 and May 2017, scarp scales along the nine profiles decreased gradually from 1.3 m to 0.6 m. When the first post-nourishment energetic storm, i.e., Typhoon Hato, approached in August 2017, all the scarps disappeared. Then, nearly three years since, scarps did not appear although two other energetic storms approached.
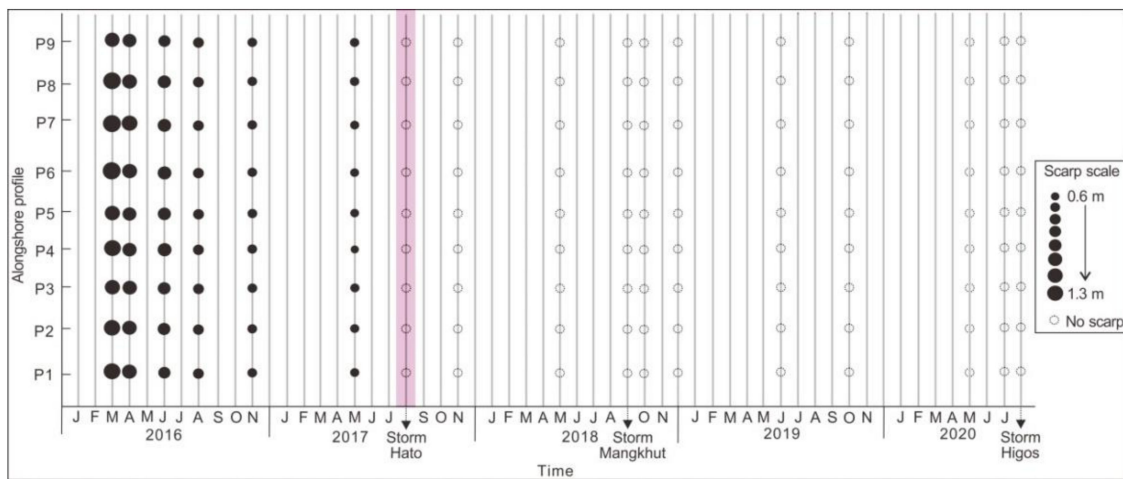

Figure 8. Temporal distribution of scarp occurrence and absence along ML beach. Grey vertical lines show the temporal variation in months while lines inlayed with circles highlight the conducted field surveys. Solid circles indicate beach scarp presence with their radius representing scarp height, while hollow circles represent beach scarp absence. Pink band highlights the period in which scarps are removed fully from ML beach.

4.3. Beach Slope Changes

For the first survey after nourishment in March 2016, ML beach showed generally steep upper beach slopes due to the formation of scarps, in contrast to the much gentler middle beach slopes. Between March 2016 and May 2017, upper beach slopes decreased gradually with the landward retreat of scarps. However, they dropped sharply when Typhoon Hato made its landfall in August 2017, with the average dropping from 0.30 to approximately 0.06 (Figure 9a). In the nearly three years since, the upper beach slopes along ML beach remained relatively stable, ranging from 0.04 to 0.07. They did not change despite the two other energetic storms that approached in September 2018 and August 2020. Different from the variation pattern of the upper beach slopes, the middle beach slopes along ML beach showed a slight variation with time (Figure 9b). They generally varied between 0.09 and 0.13, which was obviously larger than the upper beach slopes post-Hato (ranging from 0.04 to 0.07). It was also delineated that the middle beach slopes showed invisible responses to the three severe storms.
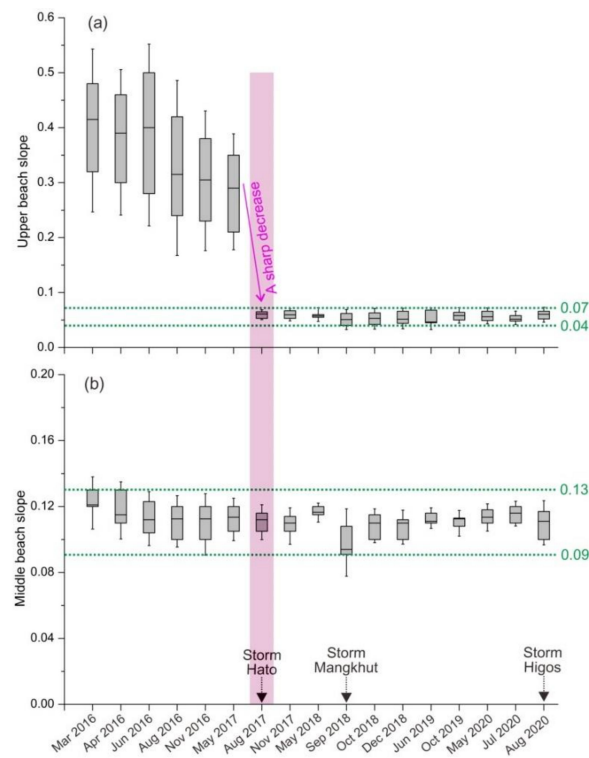
Figure 9. Temporal evolution of upper (**a**) and middle beach slopes (**b**) along ML beach during the study period. Pink band highlights the period when a sharp decrease in the upper beach slope occurs. Note that the horizontal axis shows irregular intervals between two successive surveys.

4.4. Runup and Total Water Level

Although a time-series variation of wave runup was unavailable, the upper limit of runup can be estimated from the largest wave heights. At ML beach, both of the observed (Figures 2b and 5) and simulated significant wave heights (Figure 4) were smaller than 1.0 m during normal weather (non-storm weather). According to Stockdon et al. [25], the calculated wave runup ($R_{2\%}$) was less than 0.7 m.

Furthermore, based on the difference between the observed water levels and astronomical tidal levels, wave setup or storm surge could be estimated. It was indicated that wave setup at ML beach was smaller than 0.5 m during normal weather (Figure 10). Therefore, the total water level (η) under normal weather condition was no more than 2.4 m (1.2 m (astronomical spring high tidal level) +0.5 m (wave setup) +0.7 m (wave runup)), which was much lower than the berm height (3.0 m).
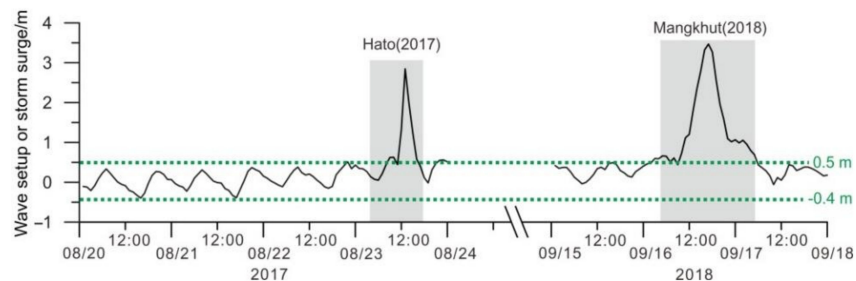

Figure 10. Time-series variation of wave setup or storm surge along ML beach during Typhoon Hato (2017) and Mangkhut (2018). Grey bands highlight the period in which storms induced significant surges.

5. Discussion

5.1. Mechanism of Scarp Formation, Migration, Destruction and Long-Term Absence

Time-series observation of beach scarps along ML beach showed that beach scarps were generally developed after nourishment. Previous studies showed that scarp heights depend on the difference between the nourishment berm height and hydrodynamic conditions [3,5,7]. At ML beach, the nourished beach berm was 3.0 m in elevation, which was much higher than the maximum total water level (2.4 m) under normal weather. At high water levels, wave energy dissipated completely and the backflow took away part of the sediment on foreshore, leading to the formation of a steep scarp in the seaward of the berm (Figure 11a). It showed that the formation of beach scarps at ML beach was attributed to the much higher designed berm, which was also confirmed by Dean and Dalrymple [15] and Jackson et al. [12] who found that an inadequate design of the nourished beach profile could lead to the formation of beach scarps.
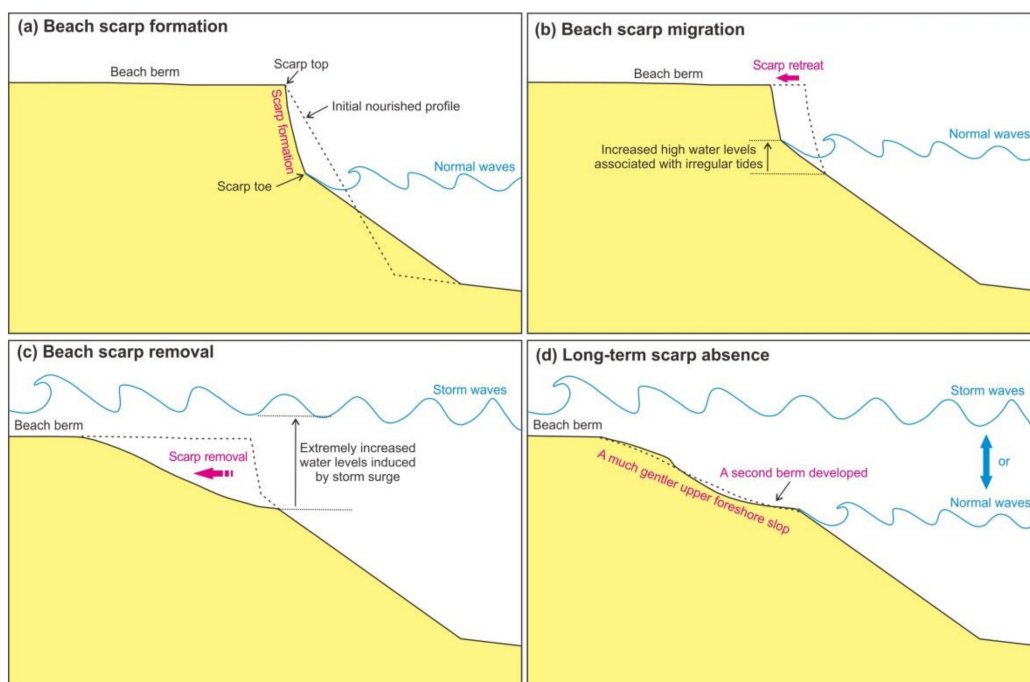

Figure 11. Four phases of beach scarp evolution for a nourished beach in low-energy and micro-tidal environment; beach scarp formation (**a**), beach scarp migration (**b**), beach scarp removal (**c**), and long-term scarp absence (**d**).

Following the formation of scarps, landward migration was observed, which was possibly attributed to the increasing high water levels associated with irregular tides. Previous scarp toe was exceeded by the subsequent wave runup and then migrated landward initiated by undercutting and slumping [6,26]. With its landward migration, the elevation of scarp toe increased gradually, companied by the reduction of their dimension (Figure 11b).

The observation also showed that all beach scarps were completely removed along ML beach after Typhoon Hato. During Hato, the total water level induced by the storm surge was approximately 3.7 m, which was much higher than the berm height (3.0 m), leading to the smoothing of the upper beach and complete removal of beach scarps (Figure 11c). Scarp destruction during storms was also observed by Bonte and Levoy [6], van Bemmelen [26], and Martell et al. [27]. This type of destruction mechanism corresponded to the inundation regime described by van Bemmelen et al. [3]. It was highlighted that the destruction of beach scarps along ML beach was closely related to severe storm conditions. In other words, the time scale of scarp presence depends on the time when the first storm approaches after nourishment, which was consistent with the findings of Jackson et al. [12] and Larson et al. [14].

The long-term observation at ML beach also showed that beach scarps had been no longer present in the nearly three years since the first post-nourishment storm (Typhoon Hato) although two other energetic storms approached. This finding was completely different from the result of van Bemmelen et al. [3], Jackson et al. [12], and de Schipper et al. [16] that beach scarps still formed after storms at nourished beaches. This was possibly connected with the gentle upper beach slope since the first post-nourishment storm. Immediately after Hato, the upper beach slopes decreased sharply from 0.30 to 0.06 (Figure 9a), combined with the berm changing from horizontal to gently sloping. During the nearly three years since Hato, the upper beach slopes ranged from 0.04 to 0.07, which was much gentler than the middle beach slope (0.09–0.13) (Figure 9). This gentle slope had impeded the formation of beach scarps since scarp formation was often connected to steep foreshore slopes [3,5]. Instead, a secondary berm gradually developed at the elevation of the mean high water (Figure 11d).

The above four phases depicted the full process of beach scarp evolution for a nourished beach in low-energy and micro-tidal environment (Figure 11). The four phases respectively corresponded to the four stages of profile equilibration for nourished beaches characterized by a low-energy wave and a small tidal range environment, proposed by Liu et al. [21]. From the comparison between the four phases of beach scarp evolution and four stages of profile equilibration, it could also be concluded that the evolution of scarps determined the process of profile equilibration.

5.2. Implications for Beach Nourishment

Beach nourishment involves the placement of large volumes of sand along the beach profile. During construction, the dredging sand are usually placed at a slope steeper than the natural beach slope because it is cost prohibitive to shape the beach profile beyond the area where the waves are breaking [28]. After construction, natural forces, such as waves and currents, move the sand offshore and soften the slope. However, beach scarps are likely to form within these systems due to the generally steep cross-shore profiles associated with beach nourishments [26]. The berm height determines the scarp top while the scarp toe elevation is strongly connected to the maximum runup elevation [6]. Therefore, the scarp height depends on the difference between the nourishment berm height and hydrodynamic conditions [3]. If the berm is designed too high, larger scarps will probably occur and persist for a long period. In addition, it may take a considerably longer time before the beach returns to its natural state [14]. Therefore, in beach nourishment projects, the berm should be designed scientifically and properly.

However, there are no universal rules to determine berm height in beach nourishment projects. According to China's experiences, two methods have been widely used [29]. The first method is to reference the berm height at the original beach before nourishment or adjacent natural beaches. These beaches have long been interacted with local hydrodynamics, their berms are naturally formed and thus considered as the natural template for artificial berms. This method is appropriate for nourishment cases where there are natural beaches nearby. The other is the empirical formula method basing on the tidal level and wave runup, which can be estimated as:

$$E_b = E_{1/20} + R_{2\%} \tag{2}$$

where E_b is the berm height, $E_{1/20}$ is the high water level in twenty-year return period, and $R_{2\%}$ is the 2% exceedance wave runup. This method is more appropriate for nourishment cases where there is no natural beach. The above two methods of determining berm elevation can be helpful for other countries' beach nourishment projects.

6. Conclusions

This study investigated the formation, migration, destruction, and long-term elimination of beach scarps at a nourished beach along a low-energy and micro-tidal coast. Based on the beach topography observation at ML beach, it was found that scarps formed

extensively after nourishment. The formation of beach scarps was attributed to the higher designed berm and relatively steep beach slopes. Following the formation of scarps, migration was possibly initiated by the subsequent higher total water level connected with irregular tides. Scarp destruction was related to severe storm conditions with the inundation regime mechanism. The results also demonstrated a surprising finding that beach scarps had been long absent since the first post-nourishment storm although two other energetic storms approached, which was attributed to the gentle upper beach slope. These results highlighted that the first post-nourishment storm played a key role in the evolution of beach scarps at low-energy and micro-tidal nourished beaches.

In beach nourishment projects, the berm should be designed scientifically and properly. Two methods of determining berm elevation were proposed according to China's experiences, which would be helpful for other countries' beach nourishment projects.

References

1. Sherman, D.; Nordstrom, K.F. Beach scarps. *Z. Geomorphol.* **1985**, *29*, 139–152.
2. Jackson, N.L.; Smith, D.R.; Nordstrom, K. Comparison of sediment characteristics on nourished and unnourished estuarine beaches in Delaware Bay, New Jersey. *Geomorphology* **2005**, *141*, 31–45.
3. Van Bemmelen, C.; De Schipper, M.; Darnall, J.; Aarninkhof, S. Beach scarp dynamics at nourished beaches. *Coast. Eng.* **2020**, *160*, 103725. [CrossRef]
4. Nishi, R.; Sato, M.; Wang, H. Field observation and numerical simulation of beach and dune scarps. In Proceedings of the 24th Coastal Engineering Conference 1994, ASCE, Kobe, Japan, 23–28 October 1994; pp. 2434–2448. [CrossRef]
5. De Alegria-Arzaburu, A.R.; Mariño-Tapia, I.; Silva, R.; Pedrozo-Acuña, A. Post-nourishment beach scarp morphodynamics. *J. Coast. Res.* **2013**, *65*, 576–581. [CrossRef]
6. Bonte, Y.; Levoy, F. Field experiments of beach scarp erosion during oblique wave, stormy conditions (Normandy, France). *Geomorphology* **2015**, *236*, 132–147. [CrossRef]
7. Van Gaalen, J.F.; Kruse, S.E.; Coco, G.; Collins, L.; Doering, T. Geomorphology observations of beach cusp evolution at Melbourne beach, Florida, USA. *Geomorphology* **2011**, *129*, 131–140. [CrossRef]
8. Vousdoukas, M.; Almeida, L.; Ferreira, O. Modelling storm-induced beach morphological change in a meso-tidal, reflective beach using XBeach. *J. Coast. Res.* **2011**, *64*, 1916–1920.
9. Anfuso, G.; Benavente, J.; Gracia, F.J. Morphodynamic responses of nourished beaches in SW Spain. *J. Coast. Conserv.* **2001**, *7*, 71–80. [CrossRef]
10. Seymour, R.; Guza, R.; O'Reilly, W.; Elgar, S. Rapid erosion of a small southern California beach fill. *Coast. Eng.* **2005**, *52*, 151–158. [CrossRef]
11. Elko, N.A.; Wang, P. Immediate profile and planform evolution of a beach nourishment project with hurricane influences. *Coast. Eng.* **2007**, *54*, 49–66. [CrossRef]
12. Jackson, N.L.; Nordstrom, K.F.; Saini, S.; Smith, D.R. Effects of nourishment on the form and function of an estuarine beach. *Ecol. Eng.* **2010**, *36*, 1709–1718. [CrossRef]

13. De Zeeuw, R.; De Schipper, M.A.; Roelvink, D.; De Vries, S.; Stive, M.J.F. Impact of nourishments on nearshore currents and swimmer safety on the Dutch Coast. *Coast. Eng. Proc.* **2012**, *1*, 12. [CrossRef]

14. Larson, M.; Hanson, H.; Kraus, N.C.; Newe, J. Short- and Long-Term Responses of Beach Fills Determined by EOF Analysis. *J. Waterw. Port. Coastal Ocean. Eng.* **1999**, *125*, 285–293. [CrossRef]

15. Dean, R.G.; Dalrymple, R.A. *Coastal Processes with Engineering Applications*; Cambridge University Press: Cambridge, UK, 2004; p. 476.

16. De Schipper, M.A.; Darnall, J.; de Vries, S.; Reniers, A.J.H.M. Beach scarp evolution and prediction. In Proceedings of the Coastal Dynamics 2017, Helsingør, Denmark, 12–16 June 2017; pp. 791–800.

17. Neshaei, M.A.L.; Ghanbarpour, F. The effect of sea level rise on beach morphology of Caspian Sea Coast. *Front. Struct. Civ. Eng.* **2017**, *11*, 369–379. [CrossRef]

18. Qi, H.; Cai, F.; Lei, G.; Cao, H.; Shi, F. The response of three main beach types to tropical storms in South China. *Mar. Geol.* **2010**, *275*, 244–254. [CrossRef]

19. Lei, G.; Zhu, J.; Cao, H.; Zheng, J.; Liu, J. *Engineering Feasibility Study Report on the Beach Nourishment Project at Meili Bay in Zhuhai City*; Third Institute of Oceanography, State Oceanic Administration: Xiamen, China, 2015. (In Chinese)

20. Pranzini, E.; Anfuso, G.; Muñoz-Perez, J.J. A probabilistic approach to borrow sediment selection in beach nourishment projects. *Coast. Eng.* **2018**, *139*, 32–35. [CrossRef]

21. Liu, G.; Cai, F.; Qi, H.; Zhu, J.; Liu, J. Morphodynamic evolution and adaptability of nourished beaches. *J. Coast. Res.* **2019**, *35*, 737. [CrossRef]

22. Chen, Y.; Chen, L.; Zhang, H.; Gong, W. Effects of wave-current interaction on the Pearl River Estuary during Typhoon Hato. *Estuar. Coast. Shelf Sci.* **2019**, *228*, 106364. [CrossRef]

23. ESCAP/WMO Typhoon Committee. Member Report (China). In Proceedings of the 12th Integrated Workshop, Jeju, Korea, 30 October–3 November 2017. Available online: http://www.typhooncommittee.org/12IWS/docs/Members/China20171026_final.pdf (accessed on 10 November 2020).

24. Yang, J.; Li, L.; Zhao, K.; Wang, P.; Wang, D.; Sou, I.M.; Yang, Z.; Hu, J.; Tang, X.; Mok, K.M.; et al. A comparative study of Typhoon Hato (2017) and Typhoon Mangkhut (2018)—Their impacts on coastal inundation in Macau. *J. Geophys. Res. Oceans* **2019**, *124*, 9590–9619. [CrossRef]

25. Stockdon, H.F.; Holman, R.A.; Howd, P.A.; Sallenger, A.H. Empirical parametererization of setup, swash and runup. *Coast. Eng.* **2006**, *53*, 573–588. [CrossRef]

26. Van Bemmelen, C.W.T. Beach Scarp Morphodynamics: Formation, Migration, and Destruction. Master's Thesis, Delft University of Technology, Delft, The Netherlands, 26 February 2018.

27. Martell, R.; Mendoza, E.; Mariño-Tapia, I.; Odériz, I.; Silva, R. How effective were the beach nourishments at Cancun? *J. Mar. Sci. Eng.* **2020**, *8*, 388. [CrossRef]

28. Willson, K.; Thomson, G.; Briggs, T.R.; Elko, N.; Miller, J. Beach nourishment profile equilibration: What to expect after sand is placed on a beach (ASBPA white paper). *Shore Beach* **2017**, *85*, 49–51.

29. Cai, F.; Liu, J.; Qi, H.; Cao, H.; Lei, G.; Zhang, C.; Zhu, J.; Yu, F. *Technical Guide for Beach Nourishment and Restoration*; Ministry of Natural Resources: Beijing, China, 2018. (In Chinese)